Journal of Power Sources 266 (2014) 193–197

Contents lists available at ScienceDirect

Journal of Power Sources

journal homepage: www.elsevier.com/locate/jpowsour

Short communication

Influence of cationic structures on oxygen reduction reaction at Pt electrode in fluorohydrogenate ionic liquids

Pisit Kiatkittikul, Jumpei Yamaguchi, Ryosuke Taniki, Kazuhiko Matsumoto, Toshiyuki Nohira*, Rika Hagiwara

Department of Fundamental Energy Science, Graduate School of Energy Science, Kyoto University, Sakyo-ku, Kyoto 606-8501, Japan

HIGHLIGHTS

- ORR on Pt electrode was evaluated in various fluorohydrogenate ionic liquids.
- The largest kinetically limited current was observed in $EMPyr(FH)_{1.7}F$.
- Low yield of H_2O_2 (about 1.9%) was observed in $EMPyr(FH)_{1.7}F$.
- Diffusion coefficients and solubilities of oxygen in various ionic liquids were determined.
- The estimated crossover currents of oxygen were small enough for practical use.

ARTICLE INFO

Article history:
Received 15 February 2014
Received in revised form
19 April 2014
Accepted 4 May 2014
Available online 14 May 2014

Keywords:
Ionic liquid
Fluorohydrogenate
Oxygen reduction reaction
Fuel cell

ABSTRACT

Various parameters related to the oxygen reduction reaction (ORR) on a Pt electrode such as kinetically limited current density (j_k), yield of H_2O_2 ($X_{H_2O_2}$), and solubility (C) and diffusion coefficient (D) of oxygen were evaluated at 298 K in fluorohydrogenate ionic liquids (FHILs) using the rotating ring-disk electrode (RRDE) method. The FHILs investigated in this study were 1-ethyl-3-methylimidazolium fluorohydrogenates ($EMIm(FH)_{1.3}F$ and $EMIm(FH)_{2.3}F$), *N*-ethyl-*N*-methyl pyrrolidinium fluorohydrogenates ($EMPyr(FH)_{1.7}F$ and $EMPyr(FH)_{2.3}F$), trimethylsulfonium fluorohydrogenate ($S_{111}(FH)_{1.9}F$), triethyl-*n*-pentylphosphonium fluorohydrogenate ($P_{2225}(FH)_{2.1}F$), and 5-azoniaspiro[4.4]nonane fluorohydrogenate ($AS[4.4](FH)_{2.0}F$). Among them, $EMPyr(FH)_{1.7}F$ showed the largest j_k value (-1.5 mA cm^{-2}) at 0.7 V vs. RHE. $EMPyr(FH)_{1.7}F$, $EMPyr(FH)_{2.3}F$, and $P_{2225}(FH)_{2.1}F$ showed small $X_{H_2O_2}$ values around 1.5% at a disk electrode potential of 0.2 V vs. RHE. The C and D values obtained for the FHILs were in the ranges of 0.23–1.3 mmol dm^{-3} and (1.1–3.2) $\times$ 10^{-5} cm^2 s^{-1}, respectively. The crossover currents of oxygen in the FHILs were estimated using the obtained C and D values, which were of the same order of magnitude as that for a 0.5 M H_2SO_4 aqueous solution.

1. Introduction

The conventional perfluorosulfonate membranes used for polymer electrolyte fuel cells (PEFCs) such as Nafion® require humidification because high proton conduction is only possible when these membranes are in the hydrated state. Thus, the practical operation temperature of conventional PEFCs is limited to below 353 K. On the other hand, unhumidified operation of PEFCs above 373 K has many advantages; (1) lower cost resulting from the smaller amount of platinum catalyst by the reduction of cathode overpotential, (2) more compact system with no humidifier and smaller radiator, and (3) higher total energy efficiency by the efficient use of waste heat. Therefore, developments of membrane electrolytes that can be used at intermediate temperatures without humidification are very desirable.

Several approaches have been used for the operation of PEFCs above 353 K including the introduction and modification of the cell with perfluorosulfonic acid polymer membranes [1–4], sulfonated hydrocarbon polymer membranes [5–8], acid–base complex membranes [9–11] and polybenzimidazole-based polymer membranes [12–15]. Such proton conductors, however, still exhibit a number of problems, for example, insufficient mechanical properties, and a narrow operational temperature range.

* Corresponding author. Tel.: +81 75 753 5827; fax: +81 75 753 5906.
E-mail address: nohira@energy.kyoto-u.ac.jp (T. Nohira).

http://dx.doi.org/10.1016/j.jpowsour.2014.05.019
0378-7753/

Polymer membranes that rely on room-temperature ionic liquids (RTILs) have recently attracted considerable attention because of their unique properties that include low volatility, high chemical and thermal stabilities, and a wide electrochemical window [16–24]. Fluorohydrogenate ionic liquids (FHILs) possess high ionic conductivity and a wide liquid-phase temperature range, which make them favorable as electrolytes for PEFC [25–32]. FHILs contain fluorohydrogenate anions ($(FH)_nF^-$, where n represents the average composition of HF in the anion) as the anionic species. Evacuation of FHILs at higher temperature reduces their n values.

Fluorohydrogenate fuel cells (FHFCs) are fuel cells using FHILs as the electrolytes to generate electrical power through the process of fluorohydrogenate anion conduction [33]. Since FHFCs are not based on the conventional proton conduction mechanism that takes place in the presence of water, they do not require humidification. This enables them to operate at higher temperatures. The cell reactions in FHFC can be expressed as follows:

For $2 < n < 3$ in $(FH)_nF^-$,

$$\text{Anode:} \quad H_2 + 8(FH)_2F^- \rightarrow 6(FH)_3F^- + 2e^- \tag{1}$$

$$\text{Cathode:} \quad 1/2O_2 + 6(FH)_3F^- + 2e^- \rightarrow H_2O + 8(FH)_2F^- \tag{2}$$

$$\text{Total:} \quad H_2 + 1/2O_2 \rightarrow H_2O \tag{3}$$

For $1 < n < 2$ in $(FH)_nF^-$,

$$\text{Anode:} \quad H_2 + 6FHF^- \rightarrow 4(FH)_2F^- + 2e^- \tag{4}$$

$$\text{Cathode:} \quad 1/2O_2 + 4(FH)_2F^- + 2e^- \rightarrow H_2O + 6FHF^- \tag{5}$$

$$\text{Total:} \quad H_2 + 1/2O_2 \rightarrow H_2O \tag{6}$$

In the first report on FHFCs, $EMIm(FH)_nF$ ($EMIm^+$: 1-ethyl-3-methylimidazolium, n = 1.3 and 2.3), was used as an electrolyte [33]. FHFCs that use composite membranes consisting of $EMIm(FH)_{1.3}F$ and polymers demonstrate a power density of 20.2 mW cm^{-2} at 393 K [34]. Recently, FHFCs using *N*-ethyl-*N*-methyl pyrrolidinium fluorohydrogenate ($EMPyr(FH)_{1.7}F$) have also been studied, and have exhibited a maximum cell performance of 32 mW cm^{-2} [35]. FHFCs are promising as a new type of fuel cell capable of operating at intermediate temperatures without humidification. However, the cathodic overpotential is larger than the anodic overpotential for FHFCs, similar to the other conventional fuel cells [36,37]. The higher rate of the oxygen reduction reaction (ORR) is crucial for the improvement of cell performance. It was found that $EMPyr(FH)_nF$ exhibited a higher ORR activity on the Pt electrode than did the $EMIm(FH)_nF$ [37], the reason for this higher activity has not yet been clarified.

In this study, the influence of the cationic structures on the ORR parameters in FHILs has been evaluated at 298 K. The FHILs used in this study were $EMIm(FH)_{1.3}F$, $EMIm(FH)_{2.3}F$, $EMPyr(FH)_{1.7}F$, $EMPyr(FH)_{2.3}F$, trimethylsulfonium fluorohydrogenate ($S_{111}(FH)_{1.9}F$), triethyl-*n*-pentylphosphonium fluorohydrogenate ($P_{2225}(FH)_{2.1}F$), and 5-azoniaspiro[4.4]nonane fluorohydrogenate ($AS[4.4](FH)_{2.0}F$). The structures and physicochemical properties [27,28,31,32,35–38] of the FHILs used in this study are summarized in Fig. 1 and Table 1, respectively. The following ORR parameters were determined on a Pt electrode; (1) kinetically limited current density (j_k), which corresponds to the rate of ORR in the absence of any mass-transfer effects, (2) yield of H_2O_2 ($X_{H_2O_2}$) on Pt, which is the ratio of the H_2O_2 production rate to that of the overall ORR, (3) solubility (C) and diffusion coefficient (D) of oxygen in the FHILs, which correlate with the O_2 transfer ability.

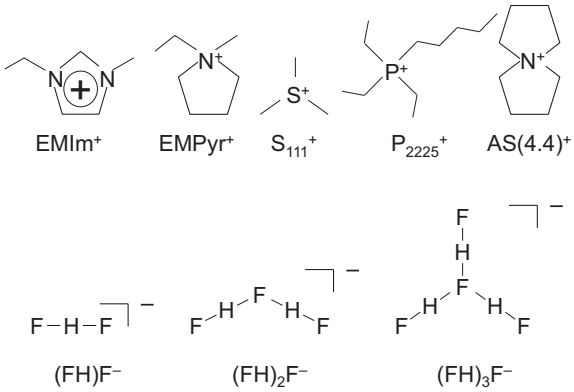

Fig. 1. Structures of cations and fluorohydrogenate anions of FHILs used in this study.

2. Experimental

$EMIm(FH)_{2.3}F$ and $EMPyr(FH)_{2.3}F$ were prepared in the manner previously reported [25,28]. An excess of anhydrous HF (Morita Chemical Industry) was distilled onto EMImCl (Yoyu Lab.) or EMPyrCl (Yoyu Lab.) at 77 K, followed by elimination of the unreacted HF and byproduct HCl at 298 K. $EMIm(FH)_{2.3}F$ and $EMPyr(FH)_{2.3}F$ were further evacuated at 393 K under reduced pressure (<1 Pa), which yielded $EMIm(FH)_{1.3}F$ and $EMPyr(FH)_{1.7}F$, respectively [33–37]. The n values of 1.3 and 1.7 were determined by elemental analyses using a CHN coder and a fluoride ion selective electrode.

Trimethylsulfonium bromide ($S_{111}Br$, Tokyo Chemical Industry Co. Ltd., >98%) was recrystallized from acetonitrile (Wako Pure Chemical Industries Co. Ltd., >99%) by adding ethyl acetate (Wako Pure Chemical Industries Co. Ltd., >99.5%) and dried under vacuum at 353 K for one day. Triethyl-*n*-pentylphosphonium bromide ($P_{2225}Br$, Nippon Chemical Industry Co. Ltd.) was dried under vacuum at 353 K for one day. The synthesis of 5-asoniaspiro[4.4] nonane bromide (AS[4.4]Br) was completed using the following typical procedure [38]. Acetonitrile, pyrrolidine (Sigma–Aldrich Co. LLC, 97%), and potassium carbonate (K_2CO_3, Wako Pure Chemical Industries Co. Ltd., >99.5%) were mixed, followed by addition of 1,4-dibromobutane (Sigma–Aldrich Co. LLC, 97%) with cooling at 273 K. The flask was connected to reflux apparatus and stirred at 333 K for 6 h. First filtration of the contents in the flask removed K_2CO_3 mostly. Addition of ethyl acetate to the filtrate resulted in recrystallization of AS[4.4]Br. After drying at 333 K for 1 day, the remaining K_2CO_3 was removed completely by passing the solution through a column filled with activated alumina. Recrystallization and washing were repeated several times, followed by drying at 353 K.

$S_{111}(FH)_{1.9}F$, $P_{2225}(FH)_{2.1}F$, and $AS[4.4](FH)_{2.0}F$ were synthesized by metathesis of the bromides and anhydrous HF (Daikin Industries, >99%), which was dried over K_2NiF_6 (Ozark Mahoning), in the same

Table 1
Density (ρ), viscosity (η), and conductivity (σ) of $EMIm(FH)_{1.3}F$, $EMIm(FH)_{2.3}F$, $EMPyr(FH)_{1.7}F$, $EMPyr(FH)_{2.3}F$, $S_{111}(FH)_{1.9}F$, $P_{2225}(FH)_{2.1}F$ and $AS[4.4](FH)_{2.0}F$ at 298 K.

	ρ/g cm^{-3}	η/cP	σ/mS cm^{-1}	Refs.
$EMIm(FH)_{1.3}F$	1.17	12	33.4	[36]
$EMIm(FH)_{2.3}F$	1.13	4.9	100	[27]
$EMPyr(FH)_{1.7}F$	1.07	25	46.7	[35,37]
$EMPyr(FH)_{2.3}F$	1.07	12	74.6	[28]
$S_{111}(FH)_{1.9}F$	1.18	7.8	131	[32]
$P_{2225}(FH)_{2.1}F$	0.999	28	12.4	[31]
$AS[4.4](FH)_{2.0}F$	1.13	16	82.1	[38]

manner as for EMIm(FH)$_{2.3}$F and EMPyr(FH)$_{2.3}$F [31,32,38]. The addition and elimination of anhydrous HF were repeated several times in order to ensure the complete elimination of the bromide in the form of HBr. Since the evolution of HBr was sometimes slow, the pressure inside the closed vessel was monitored in order to ensure that the reaction had completed. $AgNO_3$ solution was used to test for the presence of residual Br^-. The product was titrated until there was no further precipitation of AgBr.

A rotating electrode system (Pine Research Instrumentation, Durham, NC) and a thermostated, three-compartment, PTFE cell were used for the electrochemical measurements. The working electrode was a rotating ring disk electrode (RRDE) consisting of a platinum disk 5.0 mm in diameter surrounded by a platinum ring with an internal diameter of 5.5 mm and an external diameter of 8.0 mm (Pine Research Instrumentation, Durham, NC). A rotating disk electrode (RDE) assembly (Pine Research Instrumentation, Durham, NC) was used to estimate the activities at Pt. Pt disk was used as the working electrodes while a Pt wire was used as the counter electrode. The reference electrode was a reversible hydrogen electrode (RHE) made of Pt-black. Electrochemical measurements were conducted with the aid of a potentio/galvanostat (IVIUMSTAT, Ivium Technologies). Dry hydrogen (purity >99.999%) was supplied from a hydrogen generator (HORIBA STEC, Co., Ltd.) at a flow rate of 10 mL min^{-1} and dry oxygen (Kyoto Teisan K. K., >99.999%) was supplied from a cylinder at the same flow rate. Prior to the electrochemical measurement, oxygen was bubbled into the cell for 2 h in order to saturate the electrolyte with O_2.

3. Results and discussion

Fig. 2 shows typical linear-sweep voltammograms for ORR on a Pt rotating disk electrode (RDE) in EMPyr(FH)$_{2.3}$F at 298 K. Cathodic currents increase as the rotating speed increases, while almost no currents are observed under nitrogen gas. From the obtained data, kinetically limited current density, j_k, was calculated using the Koutecky–Levich equation as expressed below [39–42]:

$$j^{-1} = j_k^{-1} + j_d^{-1} \quad (7)$$

$$j_d = 0.62nFD^{2/3}C\nu^{-1/6}\omega^{1/2} \quad (8)$$

where j, j_d, n, F, ν, and ω denote the observed current density, diffusion-limited current density (so-called Levich current), reaction electron number, Faraday constant, kinematic viscosity (the ratio of dynamic viscosity to the electrolyte density) and the rotating speed of the disk electrode, respectively. Fig. 3 shows the value for j_k on a Pt electrode in EMIm(FH)$_{1.3}$F, EMIm(FH)$_{2.3}$F, EMPyr(FH)$_{1.7}$F, EMPyr(FH)$_{2.3}$F, S$_{111}$(FH)$_{1.9}$F, P$_{2225}$(FH)$_{2.1}$F, and AS[4.4](FH)$_{2.0}$F at 298 K. The values of j_k at 0.7 V vs. RHE have been summarized in Table 2. Very small ORR currents were observed for EMIm(FH)$_{1.3}$F, EMIm(FH)$_{2.3}$F, and S$_{111}$(FH)$_{1.9}$F. These results may be explained by the adsorption of ILs on Pt surface. The adsorbability of these ILs onto Pt surface may be very high compared to that of other ILs. Since the active sites for ORR are occupied by the ILs, the ORR activity may be significantly low.

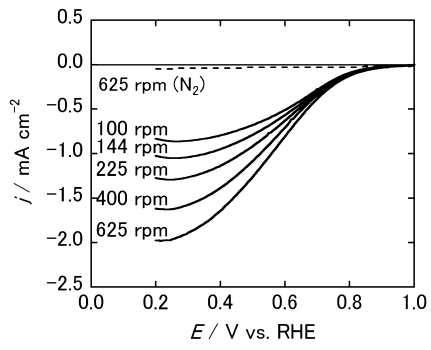

Fig. 2. Linear-sweep voltammograms for ORR on a Pt RDE in EMPyr(FH)$_{2.3}$F at 298 K. Scan rate = 10 mV s^{-1}. Rotating speed = 100–625 rpm. For comparison, the result under nitrogen atmosphere at 625 rpm is also plotted with a dashed line.

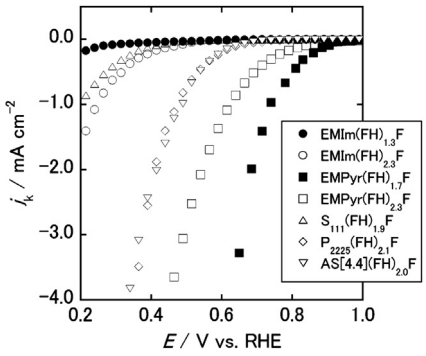

Fig. 3. Kinetically limited current densities of ORR (j_k) in EMIm(FH)$_{1.3}$F (●), EMIm(FH)$_{2.3}$F (○), EMPyr(FH)$_{1.7}$F (■), EMPyr(FH)$_{2.3}$F (□), S$_{111}$(FH)$_{1.9}$F (△), P$_{2225}$(FH)$_{2.1}$F (◇), and AS[4.4](FH)$_{2.0}$F (▽) on Pt electrodes at 298 K.

The largest j_k value of 1.5 mA cm^{-2} and the most positive onset potential (approximately 0.9 V vs. RHE) were observed in EMPyr(FH)$_{1.7}$F. This j_k value is approximately one sixth of that seen on Pt at 0.7 V vs. RHE in 0.1 M H_2SO_4 [43]. According to the study by Munakata et al. on three different protic ionic liquids based on perfluoroalkylsulfonylimides (H–N(SO$_2$(CF$_2$)$_n$F)$_2$, n = 0–2), the ORR activity depends on the degree of ion adsorption on the electrode surface [44]. By analogy, the high ORR activity found for EMPyr(FH)$_{1.7}$F may result from the much weaker adsorption of $EMPyr^+$ onto the electrode.

Tafel plots of j_k in FHILs on Pt electrodes at 298 K are shown in Supporting information, Fig. S-1. Except for EMIm(FH)$_{1.3}$F, Tafel slopes range from 0.16 V to 0.20 V, as listed in Table S-1 (supporting

Table 2
Kinetically limited current density (j_k), yield of H_2O_2 on Pt ($X_{H_2O_2}$), number of electrons associated with ORR (n), solubility (C) and diffusion coefficient (D) of oxygen, and the current density caused by oxygen crossover ($j_{crossover}$) of EMIm(FH)$_{1.3}$F, EMIm(FH)$_{2.3}$F, EMPyr(FH)$_{1.7}$F, EMPyr(FH)$_{2.3}$F, S$_{111}$(FH)$_{1.9}$F, P$_{2225}$(FH)$_{2.1}$F, AS[4.4](FH)$_{2.0}$F, 0.1 M H_2SO_4, 0.5 M H_2SO_4, Nafion®, EMImBF$_4$ and DEMATfO at 298 K, and BMPyrTFSI at 303 K.

	$\lvert j_k \rvert$[a] / mA cm^{-2}	$X_{H_2O_2}$[b] / %	n[b]	C / mmol dm^{-3}	10^6D / cm^2 s^{-1}	$j_{crossover}$[c] / mA cm^{-2}	Refs.
EMIm(FH)$_{1.3}$F	–	6.4	3.9	0.48	11	0.39	[36]
EMIm(FH)$_{2.3}$F	–	21	3.6	0.48	33	1.1	This study
EMPyr(FH)$_{1.7}$F	1.5	1.6	4.0	0.58	16	0.49	This study
EMPyr(FH)$_{2.3}$F	0.38	1.9	4.0	0.83	24	1.5	This study
S$_{111}$(FH)$_{1.9}$F	–	–	–	0.23	25	0.46	This study
P$_{2225}$(FH)$_{2.1}$F	0.033	1.2	4.0	1.3	13	1.2	This study
AS[4.4](FH)$_{2.0}$F	0.027	2.7	3.9	0.51	32	1.3	This study
0.1 M H_2SO_4	9.8	–	–	–	–	–	[44]
0.5 M H_2SO_4	–	<1	–	1.1	18	1.5	[45,51]
Nafion®[d]	–	–	–	1.4	0.58	0.063	[52]
EMImBF$_4$	–	–	–	1.1	17	0.41	[53]
DEMATfO	–	–	–	1.79	11	1.5	[54]
BMPyrTFSI[e]	0.82	–	–	2.9	12	2.6	[55]

[a] At 0.7 V vs. RHE.
[b] At 0.2 V vs. RHE.
[c] The electrolyte thickness is assumed to be 50.8 μm.
[d] Original data was measured for Nafion®117 (177.8 μm) immersed in water.
[e] At 303 K.

information). Since these values are larger than the well-known value of 0.12 V for ORR in protic electrolytes, further consideration is necessary for the elucidation of ORR mechanism for these FHILs. From the extrapolations of the Tafel plots to 1.23 V vs. RHE, the exchange current densities (j_0) were estimated, as shown in Table S-1 (supporting information). The highest j_0 of 2.2×10^{-3} mA cm^{-2} was obtained for EMPyr(FH)$_{1.7}$F. For EMIm(FH)$_{1.3}$F, it is difficult to estimate the Tafel slope and exchange current density due to the abnormal shape of the plot.

The yield of H_2O_2 ($X_{H_2O_2}$) in the ORR was determined using the rotating ring disk electrode (RRDE) method. Steady-state disk currents at 0.2 V vs. RHE and steady-state ring currents at 1.5 V vs. RHE were measured. If H_2O_2 is produced at the disk electrode in addition to H_2O, the produced H_2O_2 is oxidized at 1.5 V (see Supporting information, Fig. S-2). When a disk potential becomes more negative than 0.3 V, ring currents start increasing. $X_{H_2O_2}$/% can be calculated from the following equations [45]:

$$X_{H_2O_2}/\% = \frac{2I_R/N}{I_D + I_R/N} \times 100 \quad (9)$$

where I_D, I_R, and N denote the disk current, the ring current, and the collection efficiency, respectively. At a disk potential of 0.2 V, $X_{H_2O_2}$ was calculated to be 8.4%. It has been reported that strong adsorbates such as Cl^- and Br^- inhibit the four-electron reduction of O_2 to produce H_2O, while the two-electron reduction of O_2 to produce H_2O_2 also proceeds, resulting in high $X_{H_2O_2}$ values [46–48].

$X_{H_2O_2}$ values in EMIm(FH)$_{2.3}$F, EMPyr(FH)$_{1.7}$F, EMPyr(FH)$_{2.3}$F, P$_{2225}$(FH)$_{2.1}$F, and AS[4.4](FH)$_{2.0}$F at the Pt electrode at 298 K were also calculated, and are given together with the value for EMIm(FH)$_{1.3}$F in Table 2. As expected from their low ORR activities, EMIm(FH)$_{1.3}$F and EMIm(FH)$_{2.3}$F showed very high $X_{H_2O_2}$ values compared with other FHILs. The $X_{H_2O_2}$ values of EMIm(FH)$_{1.3}$F was 8.4% and that of EMIm(FH)$_{2.3}$F was 21%. One possible explanation for the high $X_{H_2O_2}$ values is that the adsorption of ILs on Pt surface hinders the four-electron path resulting in the low ORR activity and pushing towards the two-electron H_2O_2 path.

The $X_{H_2O_2}$ value in S$_{111}$(FH)$_{1.9}$F, however, cannot be determined due to a large anodic current corresponding to the decomposition of S$_{111}$(FH)$_{1.9}$F. Cyclic voltammograms on a Pt electrode in S$_{111}$(FH)$_{1.9}$F at 298 K under O_2 atmosphere are shown in Supporting information, Fig. S-3. In a previous report, the anodic current was not observed in such a potential region under an inert atmosphere [32]. Hence, the electrochemical stability in the positive potential region may have been changed under the oxygen atmosphere. Since a very small ORR current was observed in Fig. 3, a high $X_{H_2O_2}$ value is predicted from the same reason.

$X_{H_2O_2}$ values in EMPyr(FH)$_{1.7}$F, EMPyr(FH)$_{2.3}$F, and P$_{2225}$(FH)$_{2.1}$F were around 1.5%. These values were smaller than those observed for EMIm(FH)$_{1.3}$F, EMIm(FH)$_{2.3}$F, and S$_{111}$(FH)$_{1.9}$F and were slightly higher than those seen for the 0.5 M aqueous solution of H_2SO_4 (<1% [45]). This means that the interaction of these cations with the Pt electrode was weak, which is consistent with the large value for j_k and the positive onset potential shown in Fig. 3.

The C and D values for oxygen were determined by hydrodynamic chronocoulometry using an RDE. As a typical example, the experimental procedure and the obtained data are shown for the case of EMPyr(FH)$_{2.3}$F. Firstly, linear-sweep voltammograms were measured for ORR on a Pt RDE in EMPyr(FH)$_{2.3}$F at 298 K, as shown in Fig. 2. From the shapes of the voltammograms, the electrode reaction is regarded as diffusion-controlled at 0.2 V vs. RHE. Then, hydrodynamic chronocoulometry was conducted at this potential. Fig. 4 shows the hydrodynamic chronocoulometric curves obtained by the potential step method in which a stepwise potential was applied from the rest potential up to 0.2 V vs. RHE on a Pt RDE in

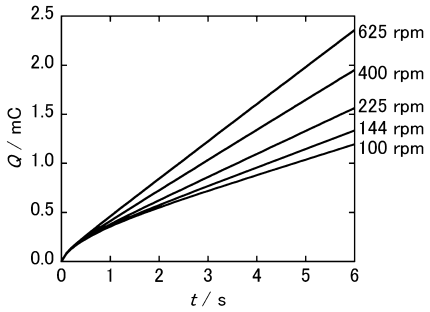

Fig. 4. Hydrodynamic chronocoulometric responses for ORR on a Pt RDE in EMPyr(FH)$_{2.3}$F at 0.2 V vs. RHE at 298 K.

EMPyr(FH)$_{2.3}$F at 298 K. There is a linear relationship between the charge, Q, and the time, t, in the region from 3 s to 5 s for both cases. According to Tsushima et al. [49], such a linear relationship can be expressed by the following equations:

$$Q = Q_{intercept} + I_d t \quad (10)$$

where $Q_{intercept}$ denotes the Q-intercept of the straight line, and I_d denotes the diffusion limited current, which corresponds to the gradient of the straight line. $Q_{intercept}$ and I_d are expressed by the following equations:

$$Q_{intercept} = 0.3764\, nFAC \times 1.610 D^{1/3} \nu^{1/6} \omega^{-1/2} \times \left(1 + 0.2980 Sc^{-1/3} + 0.1451 Sc^{-2/3}\right) + Q_{adsorption} \quad (11)$$

$$I_d = j_d A = nFADC \Big/ 1.610 D^{1/3} \nu^{1/6} \omega^{-1/2} \times \left(1 + 0.2980 Sc^{-1/3} + 0.1451 Sc^{-2/3}\right) \quad (12)$$

where $Q_{adsorption}$, A, and Sc denote the charge passed in electrolysis of the adsorbed species, the disk electrode surface area, and the Schmidt number, which is re-expressed by the ratio of the kinematic viscosity to the diffusion coefficient of O_2, respectively. The plots of j_d against $\omega^{1/2}$ and $Q_{intercept}$ against $\omega^{-1/2}$ for each FHIL are presented in Supporting information, Figs. S-4 and S-5, respectively. In the present study, the number of electrons associated with ORR, n, was calculated from $X_{H_2O_2}$ using the following equation:

$$n = 4\left(1 - \frac{X_{H_2O_2}}{100}\right) + 2\frac{X_{H_2O_2}}{100} \quad (13)$$

The values of n are listed in Table 2. For S$_{111}$(FH)$_{1.9}$F, the n value was unable to be calculated because the $X_{H_2O_2}$ value could not be determined. Thus, it was assumed to be 4 (four electron reduction) in the calculation of C.

The plots of j_d against $\omega^{1/2}$ and $Q_{intercept}$ against $\omega^{-1/2}$ show a linear relationship. From each gradient, the values of C and D were determined by combining Eqs. (11) and (12). The C and D values for EMIm(FH)$_{1.3}$F, EMIm(FH)$_{2.3}$F, EMPyr(FH)$_{1.7}$F, EMPyr(FH)$_{2.3}$F, S$_{111}$(FH)$_{1.9}$F, P$_{2225}$(FH)$_{2.1}$F, AS[4.4](FH)$_{2.0}$F are given in Table 2. It has been reported that the solubilities of hydrogen and oxygen in ionic liquids correlate with their free volumes [37,50]. Assuming that oxygen occupies the free space in ionic liquids, a smaller C value should be attributable to a smaller free volume in that ionic liquid. The smallest C value in the present FHILs is observed for S$_{111}$(FH)$_{1.9}$F, suggesting that it has the smallest free volume, which is consistent with it having the most compact ion size of S^+_{111}. On the other hand, P$_{2225}$(FH)$_{2.1}$F has the most bulky cation in the

series, giving it the largest free volume for these liquids. As a result, it exhibits the highest C value. The D values tend to decrease with increasing viscosity, which is typical for diffusion coefficients in ionic liquids. For comparison, the C and D values in 0.5 M H_2SO_4 [51], Nafion® [52], $EMImBF_4$ [53] and DEMATfO [54] at 298 K, and BMPyrTFSI [55] at 303 K are also given in Table 2. The C values obtained for the FHILs are in the region of 0.2–1.3 mmol dm^{-3} and are not much different from those for Nafion®. However, the D values are rather large in comparison with those in Nafion®, which is a solid.

The reaction electron number (n) can also be calculated by substituting the obtained C and D values in Eq. (8). For example, in the case of $EMIm(FH)_{2.3}F$, the n value was calculated to be 3.8 at 100 rpm. This value is not much different from the n value calculated from Eq. (13) using the ring data (3.6).

For the application to fuel cells, too high C and D values can cause a large amount of O_2 crossover from the cathode to the anode. On the contrary, too low C and D values hinder the supply of O_2 to the cathode. In order to evaluate the amount of O_2 crossover, the current density caused by the crossover of oxygen from cathode to anode ($j_{crossover}$) has been calculated. The following assumptions were used in this calculation: (1) the electrolyte thickness is 50.8 μm, which is equal to that of the Nafion® 212 membrane used in the present study, and (2) the reaction of the oxygen at the anode is ORR on a Pt electrode. Firstly, the permeability of oxygen (CD) was calculated. Then, the permeation rate was obtained by dividing the permeability with the thickness of electrolyte. Finally, the crossover current was calculated by multiplying the permeation rate with $4F$. The calculated $j_{crossover}$ for FHILs, 0.5 M H_2SO_4, Nafion®, $EMImBF_4$ and DEMATfO at 298 K, and BMPyrTFSI at 303 K are listed in Table 2. It has been reported that a single cell using the $EMPyr(FH)_{1.7}F$-HEMA (9:1) composite membrane exhibited a maximum current density of 150 mA cm^{-2} [35]. This value was much larger than the value calculated for $j_{crossover}$, indicating that the crossover currents are negligible for the fuel cell applications of FHILs.

4. Conclusions

In this study, the ORR was investigated in an attempt to improve the performance of fluorohydrogenate fuel cells from the viewpoint of the electrolyte. The influence of different cationic species on the ORR parameters was evaluated on a Pt electrode in $EMIm(FH)_{1.3}F$, $EMIm(FH)_{2.3}F$, $EMPyr(FH)_{1.7}F$, $EMPyr(FH)_{2.3}F$, $S_{111}(FH)_{1.9}F$, $P_{2225}(FH)_{2.1}F$, and $AS[4.4](FH)_{2.0}F$ at 298 K. The ORR parameters were kinetically limited current density (j_k), H_2O_2 yield ($X_{H_2O_2}$), solubility (C), and diffusion coefficient (D) of oxygen. $EMPyr(FH)_{1.7}F$ showed the largest j_k value that could be explained by the low adsorbability of the $EMPyr^+$ at the Pt surface as a result of the weaker interaction between $EMPyr^+$ and Pt. The $X_{H_2O_2}$ values in $EMPyr(FH)_{1.7}F$, $EMPyr(FH)_{2.3}F$, and $P_{2225}(FH)_{2.1}F$ were 1.6, 1.9, and 1.2%, respectively. The C and D values in these FHILs were considered to be appropriate for fuel cell application; the estimated crossover currents were small enough in comparison to the currents in practical use.

Acknowledgment

This work was partly supported by a Grant in Aid for Scientific Research (A) (No. 20246140) from the Japan Society for the Promotion of Science.

Appendix A. Supplementary data

Supplementary data related to this article can be found at http://dx.doi.org/10.1016/j.jpowsour.2014.05.019.

References

[1] Q. Li, R. He, J.O. Jensen, N.J. Bjerrum, Chem. Mater. 15 (2003) 4896.
[2] H. Xiuchong, T. Haolin, P. Mu, J. Appl. Polym. Sci. 108 (2008) 529.
[3] D. Wu, S.J. Paddison, J.A. Elliott, Macromolecules 42 (2009) 3358.
[4] A. Stassi, I. Gatto, E. Passalacqua, V. Antonucci, A.S. Arico, L. Merlo, C. Oldani, E. Pagano, J. Power Sources 196 (2011) 8925.
[5] S.D. Mikhailenko, S.M.J. Zaidi, S. Kaliaguine, Catal. Today 67 (2001) 225.
[6] D.X. Luu, D. Kim, J. Membr. Sci. 371 (2011) 248.
[7] A. Iulianelli, Int. J. Hydrogen Energy 37 (2012) 15241.
[8] S. Guhan, R. Muruganantham, D. Sangeetha, Can. J. Chem. 90 (2012) 205.
[9] M. Rikukawa, K. Sanui, J. Prog. Polym. Sci. 25 (2000) 1463.
[10] X. Chen, P. Chen, Z. An, K. Chen, K. Okamoto, J. Power Sources 196 (2011) 1694.
[11] Q. Tang, G. Qian, K. Huang, RSC Adv. 2 (2012) 10238.
[12] C.H. Cheng, P.C. Sui, N. Djilali, A. Su, ECS Trans. 25 (2009) 1135.
[13] D. Plackett, A. Siu, Q. Li, C. Pan, J.O. Jensen, S.F. Nielsen, A.A. Permyakova, N.J. Bjerrum, J. Membr. Sci. 383 (2011) 78.
[14] Y.C. Jin, M. Nishida, W. Kanematsu, T. Hibino, J. Power Sources 196 (2011) 6042.
[15] S.K. Kim, T. Ko, K. Kim, S.W. Choi, J.O. Park, K.H. Kim, C. Pak, H. Chang, J.C. Lee, Macromol. Res. 20 (2012) 1181.
[16] A. Noda, M.A.B.H. Susan, K. Kudo, S. Mitsushima, K. Hayamizu, M. Watanabe, J. Phys. Chem. B 107 (2003) 4024.
[17] J. Thomson, P. Dunn, L. Holmes, J.P. Belieres, C.A. Angell, D. Gervasio, ECS Trans. 13 (2008) 2821.
[18] E. Cho, J. Park, S.S. Sekhon, G. Park, T. Yang, W. Lee, C. Kim, S. Park, J. Electrochem. Soc. 156 (2009) B197.
[19] M.S. Shin, J.S. Park, J. Korean Electrochem. Soc. 15 (2012) 35.
[20] E. van de Ven, A. Chairuna, G. Merle, S.P. Benito, Z. Borneman, K. Nijmeijer, J. Power Sources 222 (2013) 202.
[21] S.Y. Lee, A. Ogawa, M. Kanno, H. Nakamoto, T. Yasuda, M. Watanabe, J. Am. Chem. Soc. 132 (2010) 9764.
[22] S.Y. Lee, T. Yasuda, M. Watanabe, J. Power Sources 195 (2010) 5909.
[23] D. Inoue, S. Mitsushima, K. Matsuzawa, S.Y. Lee, T. Yasuda, M. Watanabe, K. Ota, Electrochemistry 79 (2011) 377.
[24] T. Yasuda, S. Nakamura, Y. Honda, K. Kinugawa, S.Y. Lee, M. Watanabe, ACS Appl. Mater. Interfaces 4 (2012) 1783.
[25] R. Hagiwara, T. Hirashige, T. Tsuda, Y. Ito, J. Electrochem. Soc. 149 (2002) D1.
[26] T. Tsuda, T. Nohira, Y. Nakamori, K. Matsumoto, R. Hagiwara, Y. Ito, Solid State Ionics 149 (2002) 295.
[27] R. Hagiwara, K. Matsumoto, Y. Nakamori, T. Tsuda, Y. Ito, H. Matsumoto, K. Momota, J. Electrochem. Soc. 150 (2003) D195.
[28] K. Matsumoto, R. Hagiwara, Y. Ito, Electrochem. Solid-State Lett. 7 (2004) E41.
[29] S. Kanematsu, K. Matsumoto, R. Hagiwara, Electrochem. Commun. 11 (2007) 1312.
[30] M. Yamagata, S. Konno, K. Matsumoto, R. Hagiwara, Electrochem. Solid-State Lett. 12 (2009) F9.
[31] T. Enomoto, S. Kanematsu, K. Tsunashima, K. Matsumoto, R. Hagiwara, Phys. Chem. Chem. Phys. 13 (2011) 12536.
[32] R. Taniki, K. Matsumoto, R. Hagiwara, Electrochem. Solid-State Lett. 15 (2012) F13.
[33] R. Hagiwara, T. Nohira, K. Matsumoto, Y. Tamba, Electrochem. Solid-State Lett. 8 (2005) A231.
[34] J.S. Lee, T. Nohira, R. Hagiwara, J. Power Sources 171 (2007) 535.
[35] P. Kiatkittikul, T. Nohira, R. Hagiwara, J. Power Sources 220 (2012) 10.
[36] T. Hayashida, Master thesis of Kyoto University, 2009.
[37] Y. Tani, T. Nohira, T. Enomoto, K. Matsumoto, R. Hagiwara, Electrochim. Acta 56 (2011) 3852.
[38] R. Taniki, K. Matsumoto, R. Hagiwara, Chem. Lett. 42 (2013) 1469.
[39] A.J. Bard, L.R. Faulkner, Electrochemical Methods, Fundamentals and Applications, second ed., John Wiley & Sons, New York, 2001, p. 331.
[40] B.N. Ferdousi, Md M. Islam, T. Okajima, T. Ohsaka, Electrochim. Acta 53 (2007) 968.
[41] R. Baker, D. Wilkinson, J. Zhang, ECS Trans. 16 (2009) 43.
[42] J. Gonzalez, C. Real, L. Hoyos, R. Miranda, F. Cervantes, J. Electroanal. Chem. 651 (2011) 150.
[43] R. Halseid, T. Bystron, R. Tunold, Electrochim. Acta 51 (2006) 5737.
[44] H. Munakata, T. Tashita, M. Haibara, K. Kanamura, ECS Trans. 33 (2010) 463.
[45] U.A. Paulus, T.J. Schmidt, H.A. Gasteiger, R.J. Behm, J. Electroanal. Chem. 495 (2001) 134.
[46] N.M. Markovic, H.A. Gasteiger, B.N. Grgur, P.N. Ross, J. Electroanal. Chem. 157 (1999) 467.
[47] M. Stamenkovic, N.M. Markovic, P.N. Ross Jr., J. Electroanal. Chem. 500 (2001) 44.
[48] M.D. Maciá, J.M. Campiña, E. Herrero, J.M. Feliu, J. Electroanal. Chem. 564 (2004) 141.
[49] M. Tsushima, K. Tokuda, T. Ohsaka, Anal. Chem. 66 (1994) 4551.
[50] R. Fukuta, Y. Katayama, T. Miura, ECS Trans. 3 (2007) 567.
[51] S. Gottesfeld, I.D. Raistrick, S. Srinivasan, J. Electrochem. Soc. 134 (1987) 1455.
[52] V.A. Sethuraman, S. Khan, J.S. Jur, A.T. Haug, J.W. Weidner, Electrochim. Acta 54 (2009) 6850.
[53] Y. Katayama, H. Onodera, M. Yamagata, T. Miura, J. Electrochem. Soc. 151 (2004) A59.
[54] L. Johnson, A. Ejigu, P. Licence, D.A. Walsh, J. Phys. Chem. C 116 (2012) 18048.
[55] S. Monaco, A.M. Arangio, F. Soavi, M. Mastragostino, E. Paillard, S. Passerini, J. Electrochim. Acta 83 (2012) 94.